Aerospace Science and Technology 76 (2018) 194–203

Contents lists available at ScienceDirect

Aerospace Science and Technology

www.elsevier.com/locate/aescte

Casing grooves to improve aerodynamic performance of a HP turbine blade

Levent Ali Kavurmacioglu [a,*], Cem Berk Senel [a], Hidir Maral [a], Cengiz Camci [b]

[a] Department of Mechanical Engineering, Istanbul Technical University, Istanbul 34437, Turkey
[b] Department of Aerospace Engineering, The Pennsylvania State University, 223 Hammond Building, University Park, PA 16802, USA

ARTICLE INFO

Article history:
Received 5 June 2017
Received in revised form 2 January 2018
Accepted 12 January 2018
Available online 19 February 2018

Keywords:
Axial turbine
Casing treatment
Groove
Tip leakage flow
CFD

ABSTRACT

Highly three-dimensional and complex flow structure in the tip gap between a blade tip and the casing leads to significant inefficiency in the aerodynamic performance of a turbine. The interaction between the tip leakage vortex and the main passage flow is a substantial source of aerodynamic loss. The present research deals with the effect of groove type casing treatment on the aerodynamic performance of a linear turbine cascade. Grooved casings are widely used in compressors in order to improve the stall margin whereas limited studies are available on turbines. In this study, various circumferential grooves are investigated using the computational approach for a single stage axial turbine blade. The specific HP turbine airfoil under numerical investigation is identical to the rotor tip profile of the Axial Flow Turbine Research Facility (AFTRF) of the Pennsylvania State University. The carefully measured aerodynamic flow quantities in the AFTRF are used for initial computational quality assessment purposes. Numerical calculations are obtained by solving the three-dimensional, incompressible, steady and turbulent form of the Reynolds-Averaged Navier–Stokes (RANS) equations. A two-equation turbulence model, Shear Stress Transport (SST) k-ω is used in the present set of calculations. Current results indicate that groove type casing treatment can be used effectively in axial turbines in order to improve the aerodynamic performance. Detailed flow visualizations within the passage and numerical calculations reveal that a measurable improvement in the aerodynamic performance is possible using the specific circumferential grooves presented in this paper.

1. Introduction

A gap is required between the rotating blades and the casing in order to allow the relative motion of the blade and to prevent the blade tip surface from rubbing in most turbomachinery systems. The overall aero-thermal performance in a turbomachinery system is strongly related to the leakage flow within the tip gap. The pressure difference between the pressure side and suction side of the blade results in the tip leakage flow that is three-dimensional and highly complex. Approximately one-third of the aerodynamic losses in a rotor row is due to the leakage vortex [1]. When the leaking fluid leaves from the tip gap, it rolls up into a distinct leakage vortex and interacts with the main passage flow including the secondary flows. For this reason, highly complex flow structures appear near the blade tip and lead to inefficiency in terms of aerodynamic performance. The leakage flow also does not contribute to work generation since the flow is not turned as the passage flow [1–4]. In addition to aerodynamic aspect, the leakage flow causes higher thermal loads on the blade tip platform [4,5].

There are many studies in the literature in order to clarify the physics of the tip leakage flow and to reduce its adverse effects on the aero-thermal performance of the turbomachines. Passive control methods applied to the blade tip such as cavity squealer, partial squealer, winglet and carved designs are widely investigated in order to minimize the effects of the leakage flow and secondary flows. Heyes et al. [3] experimentally investigated the aerodynamic performance of partial squealer tips in a linear turbine cascade and obtained that suction side squealer tip geometries were effective in order to reduce the aerodynamic loss. Ameri et al. [6] performed a numerical study on the effect of a cavity squealer tip design on fluid flow and heat transfer. It was noticed that cavity squealer tip reduced the leakage flow rate whereas an increase in the total heat transfer coefficient was observed compared to the flat tip. An experimental study by Azad et al. [4] on 6 different squealer tips in a linear turbine cascade revealed that suction side squealer offered

* Corresponding author.
E-mail addresses: kavurmacio@itu.edu.tr (L.A. Kavurmacioglu), senelce@itu.edu.tr (C.B. Senel), maral@itu.edu.tr (H. Maral), cxc11@psu.edu (C. Camci).

https://doi.org/10.1016/j.ast.2018.01.047
1270-9638/

Nomenclature

Latin symbols

A	rotor passage inlet area
b	groove width
C	true chord
C_a	axial chord
C_p	pressure coefficient
C_{p0}	total pressure coefficient
D_h	hydraulic diameter (4*A/P)
g	groove depth
h	blade span
k	turbulent kinetic energy
$\dot{m}_i$	inlet mass flow rate
$\dot{m}_l$	leakage mass flow rate
M	Mach number
N	number of grooves
p	pressure
P	rotor passage inlet perimeter
p_0	total pressure
U	velocity
U_m	reference velocity
x	axial direction
y^+	dimensionless wall distance
ΔC_{p0}	total pressure loss coefficient

Greek symbols

α	flow angle
μ	dynamic viscosity
τ	tip gap height
τ/h	tip clearance
ω	specific dissipation

Abbreviations

AFTRF	Axial Flow Turbine Res. Facility
CFD	Computational Fluid Dynamics
CG	Casing Groove
LE	Leading Edge
LV	Leakage Vortex
PS	Pressure Side
RANS	Reynolds Averaged Navier Stokes
TPV	Tip Passage Vortex
TE	Trailing Edge
SS	Suction Side

better aero-thermal performance compared to cavity and pressure side squealer. Camci et al. [7] experimentally studied the aerodynamic characteristics of partial squealer rims in a single-stage, large-scale, low-speed, rotating axial flow turbine research facility (AFTRF) of the Pennsylvania State University. They found a better aerodynamic performance in the case of suction side squealer instead of cavity squealer. Key and Arts [5] compared the leakage flow characteristics of the flat and the cavity squealer tip geometries in a linear turbine cascade at low & high-speed conditions. It was measured that squealer tip designs provided lower aerodynamic loss with respect to the flat tip under specified conditions. Newton et al. [8] measured pressure coefficient and heat transfer coefficient in the tip gap for flat, suction side and cavity squealer tips in a linear cascade and supported their results with numerical computations. Their results showed that suction side and cavity squealer reduced the heat transfer to the blade tip. Kavurmacioglu et al. [9] performed detailed numerical aerodynamic calculations for a partial squealer tip and obtained a decrease in aerodynamic loss compared to flat tip. A numerical investigation on different tip geometries by Krishnababu et al. [2] indicated that cavity squealer reduced the aerodynamic loss and the heat transfer to the blade tip. Lee and Kim [10] experimentally investigated the flow structure over a cavity squealer tip design in a linear cascade turbine. Their results indicated that cavity squealer was better than flat tip in reducing the leakage flow rate. Zhou and Hodson [11] used experimental and numerical methods to study the aero-thermal performance of the cavity squealer tips and investigated the effects of the squealer width and height. Liu et al. [12] conducted a numerical investigation on the flow and the heat transfer for pressure side, suction side and cavity squealer tip geometries. The calculations revealed that cavity squealer had minimum aerodynamic loss while pressure side squealer provided minimum heat transfer to the blade tip. Schabowski and Hodson [13] found lower aerodynamic loss in the case of cavity squealer compared to the suction side squealer by their numerical and experimental studies. Ma and Wang [14] studied the aerodynamic effects of various tip designs including pressure side, suction side and cavity squealer tip geometries in a low-speed turbine cascade. Experiments showed that cavity squealer tip provided lower aerodynamic loss. Maral et al. [15] carried out a numerical investigation on the aero-thermal effects of squealer width and height of cavity squealer tips with a parametric approach.

Apart from the conventional turbine tip design approaches; there is also a passive control method, which is widely used in axial compressors in order to improve the stall margin of the turbomachine [16–20]. Studies indicate that the use of grooves that is defined as casing treatment increases the stable working condition of the compressors considerably. Grooves can be formed in different ways. Circumferential grooves correspond to the one of the most common designs. However, few studies are available on the axial turbines in the literature. To author's knowledge, the experimental study reported by Gumusel [21] is one of the limited studies that investigates the effects of casing treatment in axial flow turbines. In this study, the effect of casing treatment on over tip leakage flow was investigated in the (AFTRF). They found that the curved casing treatment in axial direction reduced the leakage flow rate and the momentum deficit in the core of the leakage vortex. Gao et al. [22] carried out a numerical investigation on the effect of a counter-rotating rotor casing to reduce the total aerodynamic losses in un-shrouded turbines using the interaction between the tip leakage vortex and the passage vortex. They concluded that the casing contouring could be used efficiently in turbines to reduce the total aerodynamic loss despite an increase in local losses.

The present research deals with the aerodynamic effects of circumferentially grooved casing treatments for a high-pressure axial turbine rotor. Different types of circumferential grooves are investigated in order to understand the flow physics in a linear cascade arrangement. Current results show that groove type casing treatment can be used effectively in axial turbines in order to improve the aerodynamic performance. Numerical calculations and numerical flow visualizations within the passage reveal that improvements in the aerodynamic performance of a turbine can be achieved using circumferential grooves.

2. Numerical method

2.1. Definition

The axial turbine blade profile and turbine operating conditions used for the computations belong to the Axial Flow Turbine Re-

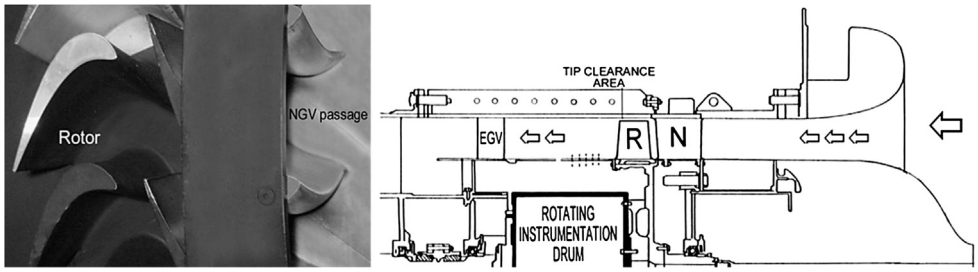

Fig. 1. Axial Flow Turbine Research Facility, AFTRF by Camci [23].

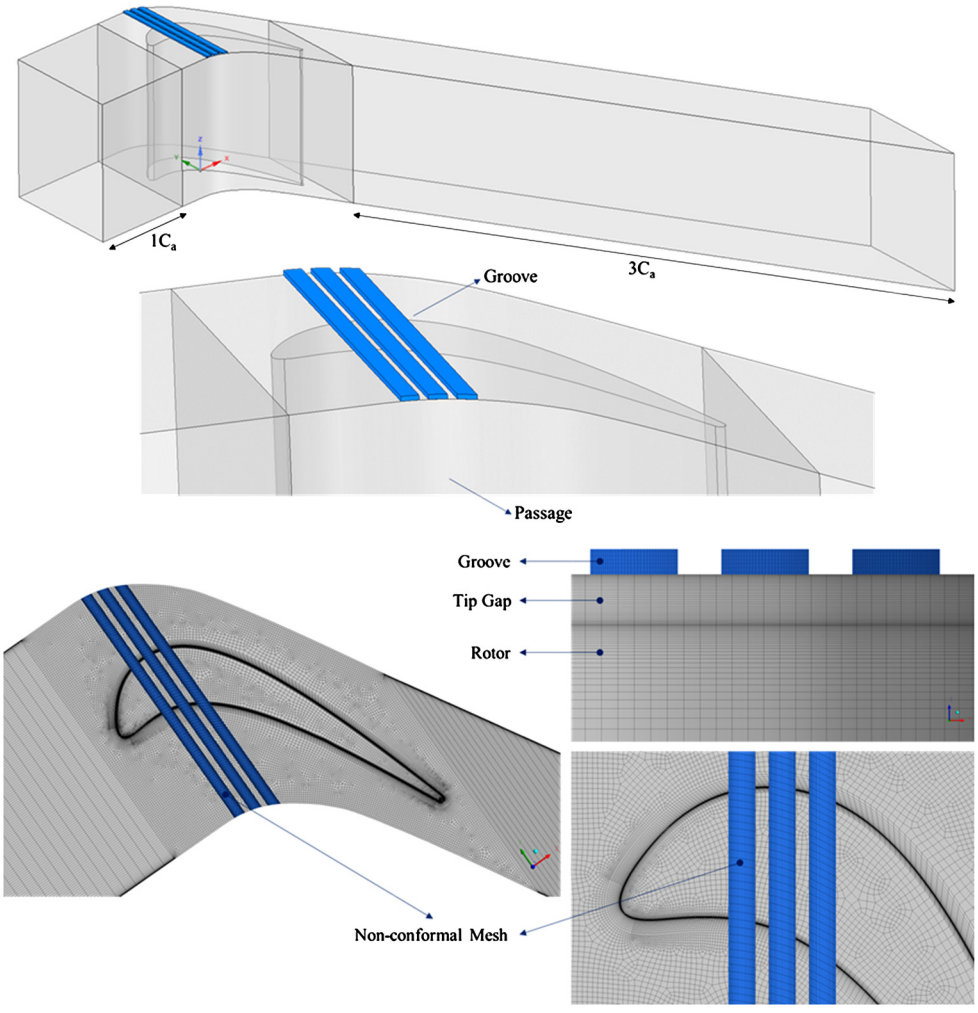

Fig. 2. Fully hexahedral grid with non-conformal interface.

search Facility (AFTRF) at the Pennsylvania State University (Fig. 1). The blade tip profile of the actual AFTRF rotor is used to create an extruded solid model of the axial turbine blade in a linear cascade arrangement. The chord based Reynolds number is calculated as 2.2×10^5 at the rotor inlet section.

The computational domain is formed as a linear turbine cascade arrangement. The blade passage with circumferential casing grooves is shown in Fig. 2. Circumferential periodicity is imposed. The design specifications of the cascade used in the current predictions are given in Table 1. Other relevant properties of the AFTRF rotor are listed in Camci [23].

The computational domain is divided into two main grid blocks as passage and groove blocks in order to perform the non-conformal grid technique (Fig. 2). The passage block consists of inlet, rotor and outlet blocks. The lengths of the inlet and the outlet block are $1.0C_a$ and $3.0C_a$ respectively. The total number of blocks in the passage block is 17.

Table 1
Design specifications of the linear turbine cascade.

Specification	Value
Blade Span, h [mm]	123
Blade Axial Chord, C_a [mm]	85.04
Blade Pitch, p [mm]	99.27
Tip Clearance, τ [mm]	2.46
Turning Angle [°]	95.42
Inlet Mass Flow Rate, $\dot{m}_I$ [kg/s]	0.38103
Inlet Re number (based on blade chord)	2.2×10^5
Zweifel coefficient (rotor)	0.9759

Creating a multi-block flow domain enabled to use the multi-zone method for grid generation in ANSYS Meshing. Multi-zone method, a type of blocking approach, uses automated topology decomposition and generates fully hexagonal grid where blocking topology is available. For the passage block, H-Grid topology is applied but in order to resolve the boundary layer around blade walls an O-Grid topology is generated to keep the y^+ value at a reasonable level. Fully hexagonal elements are used to reduce the solution time and increase the accuracy. The number of elements for the passage block is 5.9 million with 110 layers in the spanwise, 100 layers in the pitch wise and 150 layers in the streamwise direction. In order to properly capture the flow characteristics within the tip gap, 40 layers are placed in the spanwise direction. The groove grid is generated using hexagonal elements. It is appended to passage grid with non-conformal interface between two blocks (Fig. 2). Non-conformal grid method provides non-identical node locations between two adjacent interfaces and permits the cell zones to be easily connected to each other by passing fluxes from one mesh to another. Thus, different types of groove grids could be generated with significant time savings.

2.2. Boundary conditions and solver setup

Boundary conditions are obtained from the AFTRF test rig measurements [23]. Mass flow inlet and static pressure outlet boundary conditions are imposed at rotor inlet and exit sections. The AFTRF related inlet mass flow rate imposed in the current computations is obtained from a measured inlet mean velocity profile as shown in Fig. 4(b). Further information about the rotor inlet boundary conditions could be obtained from Turgut and Camci [24]. At turbine inlet, turbulence intensity and hydraulic diameter are defined as 0.5% and $D_h = 0.11$ m respectively. Maximum Mach number in the computational domain is such that the compressibility effects are neglected ($M < 0.3$). No-slip and adiabatic conditions are applied on all cascade walls. Periodicity in the pitch wise direction is imposed and the casing is modeled as a stationary endwall. Numerical calculations are performed by solving the 3D, incompressible, steady and turbulent form of the Reynolds-Averaged Navier–Stokes (RANS) equations by introducing a finite volume discretization using the commercial code ANSYS Fluent 16.0. A fully turbulent flow is assumed throughout the computations. Pressure based coupled algorithm is used for pressure-velocity coupling. Flow in the tip gap has highly swirling character, so "Pressure Staggering Option" scheme is used for the pressure discretization. For the discretization of momentum, k and ω equations, a second order upwind scheme is used. The two-equation turbulence model SST k-ω is used. In order to use SST k-ω model, it is recommended to keep y^+ values smaller than 2. For all cases, y^+ is lower than the 1.5 around the blade profile at the 0.97h and its averaged value is 0.94, and therefore, y^+ condition is satisfied. The convergence level of the numerical solutions is monitored by residuals of governing equations, mass flow rate at the outlet and the total pressure loss coefficient ΔC_{p0} at $1.25C_a$. Convergence level of continuity, k and ω equations for the flat tip with and without casing groove are the order of the 10^{-3} and 10^{-4} respectively. Convergence level of velocity is the order of the 10^{-5}. The change in mass flow rate between exit and inlet is less than 0.005% at the convergence. When convergence criteria is satisfied, after 200 more iterations ΔC_{p0} at $1.25C_a$ is less than 1%.

2.3. Grid dependency test

A grid dependency study is carried out for the flat tip without casing grooves. Various grid measures in the spanwise direction along the blade span and within the tip gap is defined in Table 2.

Table 2
Grid dependency test.

Grid	Layers rotor	Layers tip gap	Number of elements	$y^+_{ave,tip}$	ΔC_{p0}	Difference % (wrt GR4)
GR1	90	24	4307820	6.5	0.2203	+1.24%
GR2	100	32	5468264	3.9	0.2166	−0.46%
GR3	110	40	5901010	2.4	0.2189	+0.60%
GR4	115	44	6268643	1.9	0.2176	–

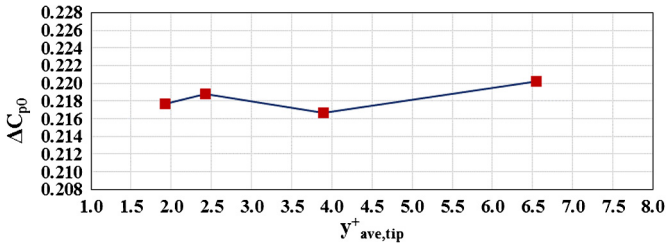

Fig. 3. ΔC_{p0} variation for different average y^+ values at blade tip surface.

From GR1 to GR4, grid structure is refined by increasing the number of layers in the rotor and tip gap regions in the spanwise direction. Accordingly, average y^+ at blade tip surface decreased from GR1 to GR4. In Fig. 3, ΔC_{p0} variation with respect to average $y^+_{ave,tip}$ values is shown. When average y^+ at the blade tip decreased from 6.5 to 1.9, the variation of ΔC_{p0} dropped below 1%. This test showed that the numerical calculations are less sensitive to the resolution of the grid. GR3 is selected as the baseline grid. Table 2 clearly shows that the selected case GR3's grid character generates a relative C_{p0} change of about 0.6% corresponding to an absolute total pressure change about 9.9 Pascal. This final value is well below a typical uncertainty accepted for experimental studies.

2.4. Validation

For the validation of the current rotor blade related computations, extensive aerodynamic measurements obtained in the nozzle guide vane passages of AFTRF by Turgut and Camci [24] are used in this paper. The validations are performed on the mid-span of the "matching NGV" of the rotor used in this study using the exact same computational solver with very similar grid characteristics. Fig. 4(a) presents the static pressure coefficient distribution C_p at the mid-span of the NGV airfoil. The computed C_p results on airfoil mid-span surfaces are in very good agreement with the experimental measurements on the matching NGV of the AFTRF stage. Moreover, the measurements of the three velocity components are plotted in Fig. 4(b) along the spanwise direction at the rotor inlet plane. The measured axial, tangential and radial velocity components are obtained by a sub-miniature five-hole probe. The figure shows a very good agreement between the numerical predictions and the experimental measurements. In addition to their validation attributes, the measured and computed velocity components at the rotor inlet as shown in Fig. 4(b) are used in the determination of the inlet boundary conditions of the rotor blade profile in the linear cascade arrangement used in this paper.

3. Aerodynamic investigation

This section provides a detailed information about predicted flow characteristics and aerodynamic performance of casing treatment in the linear cascade arrangement of the AFTRF blade defined in the previous sections. The numerical results for the flow structure of flat tip are taken as the baseline model. The aerodynamic performance of the casing treatment applications is assessed by calculating the total pressure loss coefficient, ΔC_{p0} at the exit

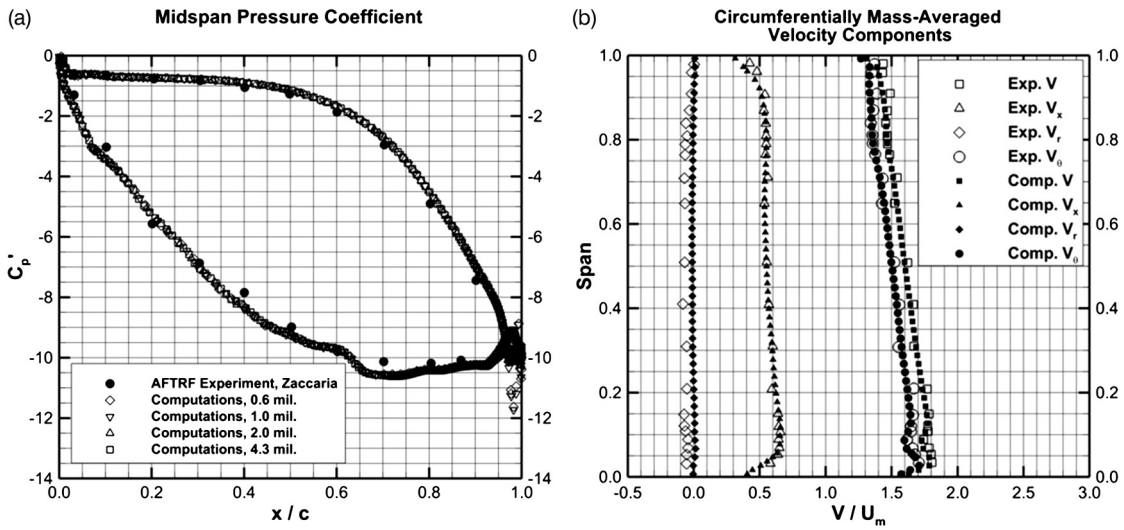

Fig. 4. Validation of the present computational approach using measured NGV aerodynamic data at AFTRF, by Turgut and Camci [24]. (a) Static pressure coefficient C_p distribution at mid-span of the NGV airfoil. (b) Comparison of the predicted axial, tangential & radial velocity components to measured velocity components.

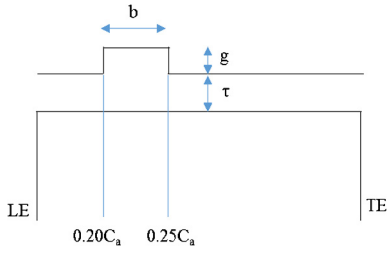

Fig. 5. Conceptual view of the single casing groove.

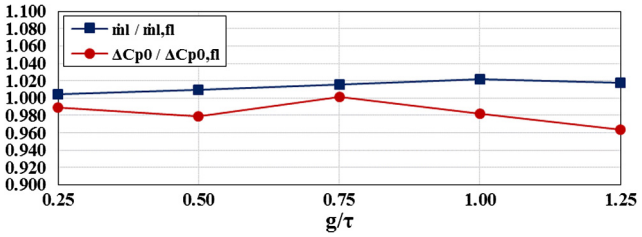

Fig. 6. $\dot{m}_l/\dot{m}_{l,fl}$ and $\Delta C_{p0}/\Delta C_{p0,fl}$ distribution related to the g/τ.

plane located at $0.25C_a$ downstream of the rotor blade trailing edge. The total pressure loss coefficient defined as,

$$\Delta C_{p0} = \frac{\iint \rho u C_{p0} dydz}{\iint \rho u dydz} \tag{1}$$

where C_{p0} is total pressure coefficient. Total pressure coefficient defined as,

$$C_{p0} = \frac{P_0 - P_{01}}{0.5\rho U_m^2} \tag{2}$$

where P_{01} is the mass averaged total pressure at the cascade inlet and U_m is the mean blade speed at the mid-span taken from AFTRF test rig. In Fig. 5 conceptual view of the single casing groove is given. The groove leading edge is located at $0.20C_a$ downstream of the blade leading edge. g and b represents the groove depth and width respectively. Tip clearance of the blade, τ/h is 2.0% for all cases, where h is blade height.

3.1. Effects of groove depth

Numerical calculations are performed for six different groove depth-to-tip gap height ratios of g/τ as 0.00, 0.25, 0.50, 0.75, 1.00 and 1.25 for a single square CG. The leakage flow rates and the total aerodynamic losses are given in Table 3 and plotted in Fig. 6. The leakage flow rate is calculated for a quantitative evaluation by forming a control surface aligned with the suction side of the blade that corresponds to the tip gap exit.

Numerical calculations indicate that the flat tip without casing grooves has the lowest leakage flow rate compared to the flat tip with casing groove. In other words, the performance of a single casing groove increased the leakage flow rate by about 1–2%. Considering that the leakage flow rate is directly related to the tip leakage loss according to Denton [25], the tip leakage loss is expected to be higher in case of higher leakage flow rates. The total aerodynamic loss in a rotor blade row can be divided into tip leakage loss, profile loss and secondary losses due to endwall boundary layer and passage vortex [26,27]. The total aerodynamic loss quantities given in Table 3 are the overall losses calculated at the exit plane. Results show that single casing grooves can improve the aerodynamic performance although tip leakage loss tends to increase due to increase in leakage flow rate. The higher leakage flow rates might be associated with increase in the tip gap at the casing groove location. The best improvement is obtained as 3.61% in the case of $g/\tau = 1.25$. However, $g/\tau = 1.25$ causes the highest leakage flow rate. Fig. 6 revealed that application of single square CG generally reduces the total aerodynamic loss compared to the flat tip without CG.

C_{p0} in the streamwise direction provides a better understanding of the flow physics of the tip leakage flow and the secondary flows. It shows the growth of the leakage vortex (LV) and secondary flow structures such as tip passage vortex (TPV) and wakes. C_{p0} also indicates the regions of momentum deficits. Fig. 7 depicts the formation of both LV and TPV at selected streamwise locations on the planes perpendicular to the camber line for 6 different **groove depth** (g/τ) values. The visualization planes are located at x = 0.27C, 0.35C, 0.43C, 0.59C, 0.77C and 0.91C. Casing grooves tend to reduce the area coverage of LV in both spanwise and pitch wise directions. The size reduction of the LV is deduced from the predicted total pressure deficit it exhibits in the vortex core. Fig. 7 shows that single square CG weakens the TPV considerably when compared to the flat tip without a groove implementation.

Fig. 8(a) shows the formation and interaction of LV and TPV on the planes located at 0.27C, 0.35C, 0.43C, 0.59C for $g/\tau = 0.00$, 0.25, 0.75 and 1.25. The TPV enlarges with groove depth and begins to interact with counter-rotating LV at 0.27C although there

Table 3
Effect of casing groove depth.

g/τ	$\dot{m}_l$	$\dot{m}_l/\dot{m}_{l,fl}$	Difference %	ΔC_{p0}	$\Delta C_{p0}/\Delta C_{p0,fl}$	Difference %
0.00	19.75	1.000	–	0.2189	1.000	–
0.25	19.83	1.004	+0.43	0.2165	0.989	−1.10
0.50	19.93	1.009	+0.94	0.2142	0.979	−2.13
0.75	20.06	1.016	+1.57	0.2191	1.001	+0.08
1.00	20.18	1.022	+2.21	0.2149	0.982	−1.82
1.25	20.10	1.018	+1.78	0.2110	0.964	−3.61

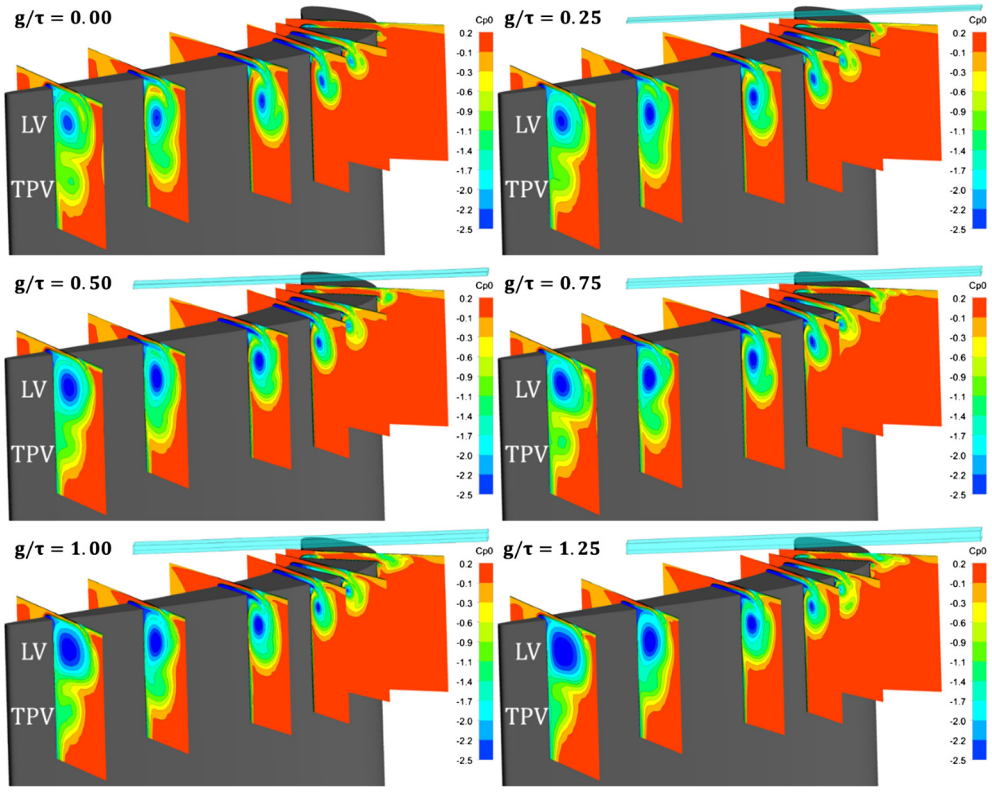

Fig. 7. Effects of groove depth on C_{p0} at various positions, 0.27C, 0.35C, 0.43C, 0.59C, 0.77C, 0.91C.

has not yet been a major interaction for the flat tip. It can be deduced that an earlier interaction between LV-TPV is observed because of the casing groove. The stronger TPV shifts the LV to the suction side, meanwhile, stronger interaction between LV and TPV weakens the TPV. As a result, this flow mechanism mitigates the momentum deficit. The weakest TPV is observed in the case of the deepest groove. The vortex core regions are presented in Fig. 8(b). The Q-criterion is used to visualize the vortex structures near the blade tip. Fig. 8(b) visually defines the vortical flow structure boundaries for comparative purposes for a set of groove depths (g/τ) values. Q-criterion is defined as the second invariant of the velocity gradient tensor and the positive values indicate the vortex regions [28]. Interactions in three-dimensional space between LV and TPV are presented in Fig. 8(b). This interaction starts earlier in the case of deep grooves compared to the flat tip. The interaction of a tip passage vortex and the leakage vortex are consistently observed in our experimental efforts in AFTRF. When tip Leakage Vortex LV grows up in size (e.g. for relatively larger tip clearance values), the Tip Passage Vortex changes its location in the passage and its total pressure deficit is reduced. For tight tip clearances with a weaker LV the Tip Passage Vortex grows in terms of its area coverage and its core has more momentum deficit. LV and TPV are inherently counter rotating vortical systems. More information about the AFTRF based experimental evidence on this interaction are given in [7], [9] and [21]. Other related information about the tip leakage flow interactions and performance issues on AFTRF tip profile are also presented in [29] and [30]. [29] deals with leakage flow patterns from conventional squealer tip arrangements. Partial and cavity type squealer flow patterns are discussed in detail in [30].

3.2. Effects of number of grooves

Numerical calculations are also performed to understand the effects of the number of grooves. The number of grooves is increased from 1 to 3 with $0.5C_a$ spacing for the square casing groove with $g/\tau = 0.50$. The reason of selection $g/\tau = 0.50$ is that it provides both lower leakage flow rate in addition to the lower overall loss compared to the $g/\tau = 1.25$. The results are given in Table 4. Leakage flow rate of the doubled CG is 0.01% lower than the flat tip without CG. The drop in aerodynamic loss compared to the flat tip without CG is 2.13%, 4.60% and 3.67% for single, doubled and tripled CG respectively. Increase in the number of grooves decreases the aerodynamic loss noticeably.

In Fig. 9, C_{p0} at x = 0.27C, 0.35C, 0.43C, 0.59C, 0.77C and 0.91C are plotted based on the number of grooves. Core of the leakage vortex becomes larger with increasing the number of grooves whereas the tip passage vortex diminishes as seen in Fig. 9. Increasing the number of grooves provided a substantial improvement in aerodynamic performance up to 4.60%. As stated earlier,

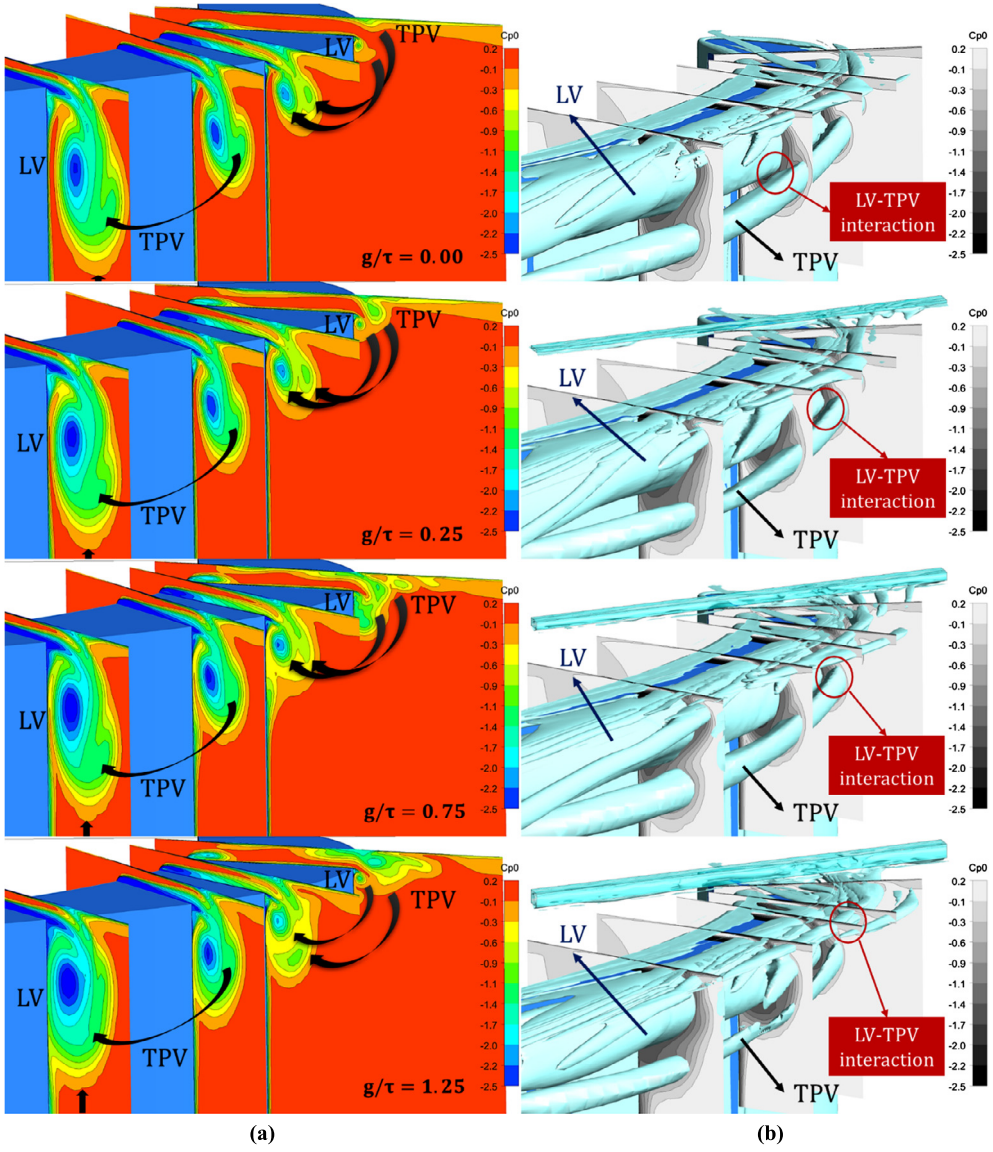

Fig. 8. (a) C_{p0} distribution. (b) Numerically visualized vortex cores using Q-criterion.

Table 4
Effects of the number of grooves.

N	$\dot{m}_l$	$\dot{m}_l/\dot{m}_{l,fl}$	Difference %	ΔC_{p0}	$\Delta C_{p0}/\Delta C_{p0,fl}$	Difference %
0	19.75		–	0.2189	1.000	–
1	19.93	1.009	+0.94	0.2142	0.979	−2.13
2	19.74	1.000	−0.01	0.2088	0.954	−4.60
3	20.00	1.013	+1.31	0.2109	0.963	−3.67

the grooves play an important role in weakening the passage vortex.

3.3. Effects of groove shape

Effect of the groove shape is also investigated for the tripled CG for square, diverged and converged shapes. The specific groove geometries are shown in Fig. 10 including the flat tip without groove. Leakage flow rate of the square CG is 1.31% higher than the flat tip without CG, whereas converged CG and diverged CG are 0.72% and 0.60 lower in Table 5. Converged CG and diverged CG could reduce the leakage flow rate unlike the previous square designs. The decrease in total aerodynamic loss compared to the flat tip without CG is 3.67%, 2.78% and 3.83% for square CG, converged CG and diverged CG respectively. From the aerodynamic loss contour plots in Fig. 11, diverged CG could reduce the size of the LV core compared to square CG and converged CG. Diverged case provides the best aerodynamic performance.

Another aerodynamic effect of tripled diverged casing groove can be seen in Fig. 12 comparing streamlines with the no casing groove case. Flow inside the casing grooves which moves in tangential direction decelerates the tip leakage flow that moves just below the casing groove flow and perpendicular to the camber line of the blade. Decelerated leakage flow has lower velocity at the tip gap exit. This leads to lower pressure gradient between pressure side and suction side of the blade tip, so the leakage flow weakens. Results listed in Table 5 confirm this observation. It indicates that

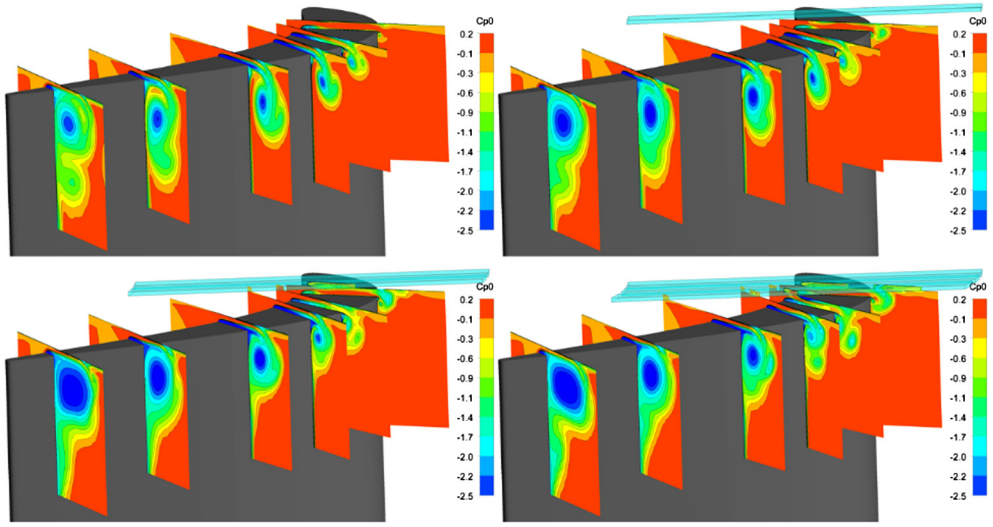

Fig. 9. Effects of the number of grooves on C_{p0} at x = 0.27C, 0.35C, 0.43C, 0.59C, 0.77C and 0.91C.

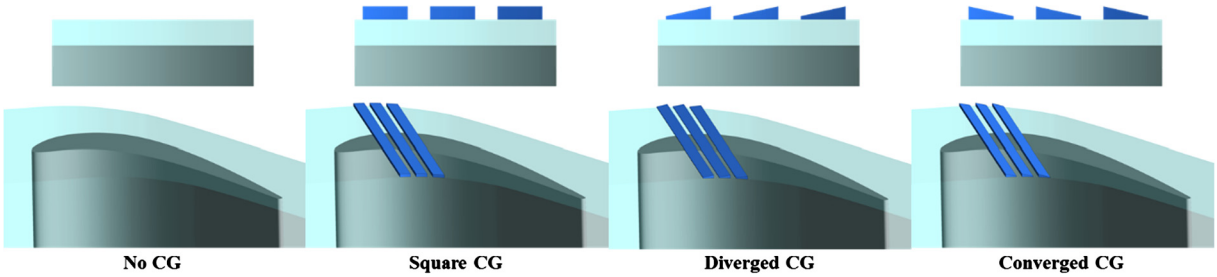

Fig. 10. The three casing groove geometries.

Table 5
Effects of casing groove shape.

Shape	$\dot{m}_l$	$\dot{m}_l/\dot{m}_{l,fl}$	Difference %	ΔC_{p0}	$\Delta C_{p0}/\Delta C_{p0,fl}$	Difference %
No CG	19.75	1.000	–	0.2189	1.000	–
Square CG	20.00	1.013	+1.31	0.2109	0.963	−3.67
Converged CG	19.60	0.993	−0.72	0.2128	0.972	−2.78
Diverged CG	19.63	0.994	−0.60	0.2105	0.962	−3.83

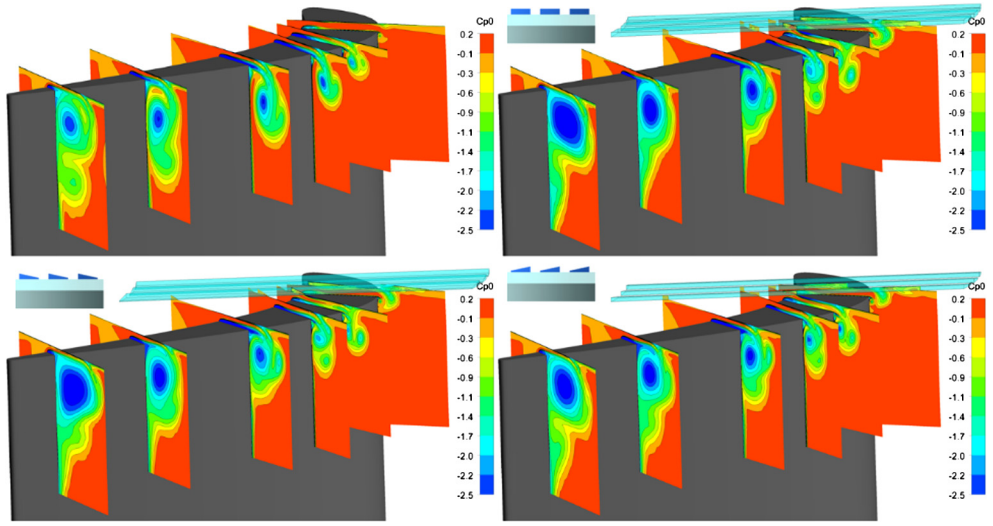

Fig. 11. Effects of groove shape on C_{p0} at 0.27C, 0.35C, 0.43C, 0.59C, 0.77C and 0.91C.

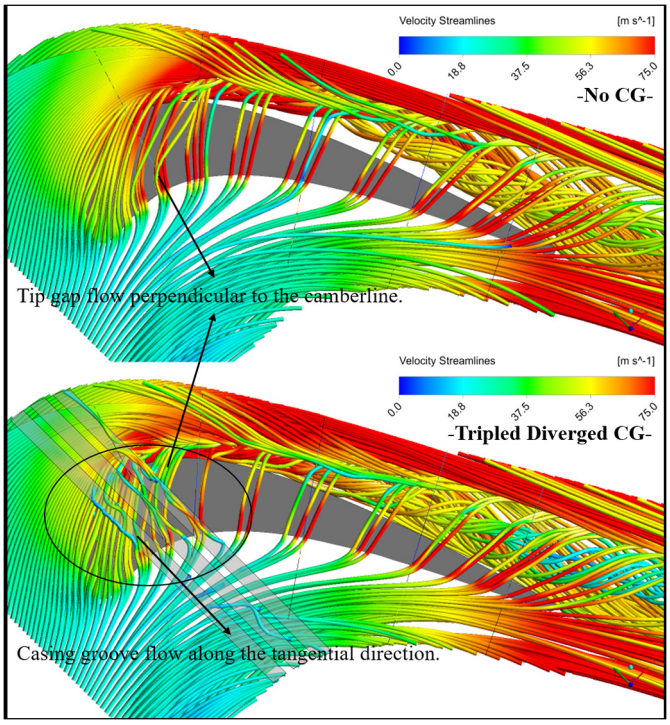

Fig. 12. Comparison of streamlines for no CG and tripled diverged CG cases.

implementation of tripled diverged casing groove could diminish both leakage flow rate and the total aerodynamic loss noticeably.

4. Conclusions

A numerical study on the effect of groove casing treatment in a linear turbine cascade is performed. Grooved casings are widely used especially in compressors in order to improve the stall margin of the turbomachine whereas limited studies are available on turbines. In this research, different types of circumferential grooves are investigated using a computational approach in a linear cascade arrangement for a turbine rotor profile. After a comprehensive evaluation and assessment of the computational system implemented, detailed information about flow physics of the casing treatment implementation are discussed. The main findings of the paper are listed as follows:

(1) An assessment of the current computational approach against comprehensive aerodynamic measurements in the specific turbine AFTRF established very good confidence for the current computations.
(2) Effects of groove depth are investigated for a single square CG. Single square CG can be affective to reduce the overall loss in spite of the increase in leakage flow rate. It weakens the passage vortex substantially when compared to the flat tip. Casing grooves reduce the size of the “Leakage Vortex” LV in both spanwise and pitch wise directions compared to the ungrooved ones. However, using a “Casing Groove” CG enlarges the core of the leakage vortex.
(3) Increasing the number of the grooves can be effectively used to reduce the total loss.
(4) Converged and diverged CG reduces both the leakage flow rate and the total loss noticeably unlike square grooves. Tripled diverged CG provides the best aerodynamic performance.
(5) Similar predictions of turbine CG configurations with the relative motion of the casing included are under progress.

Conflict of interest statement

The authors certify that they have NO affiliations with or involvement in any organization or entity with any financial interest (such as honoraria; educational grants; participation in speakers’ bureaus; membership, employment, consultancies, stock ownership, or other equity interest; and expert testimony or patent-licensing arrangements), or non-financial interest (such as personal or professional relationships, affiliations, knowledge or beliefs) in the subject matter or materials discussed in this manuscript.

Acknowledgements

This research was funded by TAI-Turkish Aerospace Industries Inc. (Grant No. DKTM/2014/05). The authors wish to thank TAI for the permission to publish this work. C. Camci also thanks to the Pennsylvania State University for its support during his sabbatical leave at Istanbul Technical University, Faculty of Mechanical Engineering.

References

[1] B. Mischo, T. Behr, R.S. Abhari, Flow physics and profiling of recessed blade tips: impact on performance and heat load, J. Turbomach. 130 (2008) 021008, https://doi.org/10.1115/1.2775485.
[2] S.K. Krishnababu, P.J. Newton, W.N. Dawes, G.D. Lock, H.P. Hodson, J. Hannis, C. Whitney, Aerothermal investigations of tip leakage flow in axial flow turbines—Part I: effect of tip geometry and tip clearance gap, J. Turbomach. 131 (2008) 011006, https://doi.org/10.1115/1.2950068.
[3] F.J.G. Heyes, H.P. Hodson, G.M. Dailey, The effect of blade tip geometry on the tip leakage flow in axial turbine cascades, J. Turbomach. 114 (1992) 643–651, https://doi.org/10.1115/1.2929188.
[4] G.S. Azad, J.-C. Han, R.S. Bunker, C.P. Lee, Effect of squealer geometry arrangement on a gas turbine blade tip heat transfer, J. Heat Transf. 124 (2002) 452–459, https://doi.org/10.1115/1.1471523.
[5] N.L. Key, T. Arts, Comparison of turbine tip leakage flow for flat tip and squealer tip geometries at high-speed conditions, J. Turbomach. 128 (2004) 213–220, https://doi.org/10.1115/1.2162183.
[6] A.A. Ameri, E. Steinthorsson, D.L. Rigby, Effect of squealer tip on rotor heat transfer and efficiency, J. Turbomach. 120 (1998) 753–759, https://doi.org/10.1115/1.2841786.
[7] C. Camci, D. Dey, L. Kavurmacioglu, Aerodynamics of tip leakage flows near partial squealer rims in an axial flow turbine stage, J. Turbomach. 127 (2005) 14–24, https://doi.org/10.1115/1.1791279.
[8] P.J. Newton, G.D. Lock, S.K. Krishnababu, H.P. Hodson, W.N. Dawes, J. Hannis, C. Whitney, Heat transfer and aerodynamics of turbine blade tips in a linear cascade, J. Turbomach. 128 (2004) 300–309, https://doi.org/10.1115/1.2137745.
[9] L. Kavurmacioglu, D. Dey, C. Camci, Aerodynamic character of partial squealer tip arrangements in an axial flow turbine. Part II: detailed numerical aerodynamic field visualisations via three dimensional viscous flow simulations around a partial squealer tip, Prog. Comput. Fluid Dyn. 7 (2007) 374–386, https://doi.org/10.1504/PCFD.2007.014960.
[10] S.W. Lee, S.U. Kim, Tip gap height effects on the aerodynamic performance of a cavity squealer tip in a turbine cascade in comparison with plane tip results: Part 1—Tip gap flow structure, Exp. Fluids 49 (2010) 1039–1051, https://doi.org/10.1007/s00348-010-0848-6.
[11] C. Zhou, H. Hodson, Squealer geometry effects on aerothermal performance of tip-leakage flow of cavity tips, J. Propuls. Power 28 (2012) 556–567, https://doi.org/10.2514/1.B34254.
[12] J.-J. Liu, P. Li, C. Zhang, B.-T. An, Flowfield and heat transfer past an unshrouded gas turbine blade tip with different shapes, J. Therm. Sci. 22 (2013) 128–134, https://doi.org/10.1007/s11630-013-0603-4.
[13] Z. Schabowski, H. Hodson, The reduction of over tip leakage loss in unshrouded axial turbines using winglets and squealers, J. Turbomach. 136 (2013) 041001, https://doi.org/10.1115/1.4024677.
[14] H. Ma, L. Wang, Experimental study of effects of tip geometry on the flow field in a turbine cascade passage, J. Therm. Sci. 24 (2015) 1–9, https://doi.org/10.1007/s11630-015-0748-4.
[15] H. Maral, C.B. Senel, L. Kavurmacioglu, A parametric and computational aerothermal investigation of squealer tip geometry in an axial turbine: a parametric approach suitable for future advanced tip carving optimizations, 2016, V02BT38A058, https://doi.org/10.1115/GT2016-58107.
[16] M. Cevik, H. Duc Vo, H. Yu, Casing treatment for desensitization of compressor performance and stability to tip clearance, J. Turbomach. 138 (2016) 121008, https://doi.org/10.1115/1.4033420.

[17] H. Chen, X. Huang, K. Shi, S. Fu, M. Ross, M.A. Bennington, J.D. Cameron, S.C. Morris, S. McNulty, A. Wadia, A computational fluid dynamics study of circumferential groove casing treatment in a transonic axial compressor, J. Turbomach. 136 (2013) 031003, https://doi.org/10.1115/1.4024651.
[18] D. Juan, L. Jichao, G. Lipeng, L. Feng, C. Jingyi, The impact of casing groove location on stall margin and tip clearance flow in a low-speed axial compressor, J. Turbomach. 138 (2016) 121007, https://doi.org/10.1115/1.4033472.
[19] N. Qin, G. Carnie, Y. Wang, S. Shahpar, Design optimization of casing grooves using zipper layer meshing, J. Turbomach. 136 (2013) 031002, https://doi.org/10.1115/1.4024650.
[20] Y. Sakuma, T. Watanabe, T. Himeno, D. Kato, T. Murooka, Y. Shuto, Numerical analysis of flow in a transonic compressor with a single circumferential casing groove: influence of groove location and depth on flow instability, J. Turbomach. 136 (2013) 031017, https://doi.org/10.1115/1.4025575.
[21] B. Gumusel, Aerodynamic and Heat Transfer Aspects of Tip and Casing Treatments Used for Turbine Tip Leakage Control, PhD thesis, The Pennsylvania State University, 2008.
[22] J. Gao, Q. Zheng, G. Yu, Reduction of tip clearance losses in an un-shrouded turbine by rotor casing contouring, J. Propuls. Power 28 (2012) 936–945, https://doi.org/10.2514/1.B34565.
[23] C. Camci, A turbine research facility to study tip desensitization including cooling flows, von Karman Institute Lecture Series, VKI-LS 2004-02, 2004, pp. 1–26, ISBN 2-930389-51-6, Brussels.
[24] Ö.H. Turgut, C. Camci, Factors influencing computational predictability of aerodynamic losses in a turbine nozzle guide vane flow, J. Fluids Eng. 138 (2016) 051103, https://doi.org/10.1115/1.4031879.
[25] J.D. Denton, The 1993 IGTI scholar lecture: loss mechanisms in turbomachines, J. Turbomach. 115 (1993) 621–656, https://doi.org/10.1115/1.2929299.
[26] M.I. Yaras, S.A. Sjolander, Prediction of tip-leakage losses in axial turbines, J. Turbomach. 114 (1992) 204–210, https://doi.org/10.1115/1.2927987.
[27] M. Zhang, Y. Liu, T.-l. Zhang, M.-c. Zhang, H.-k. Li, Aerodynamic optimization of a winglet-shroud tip geometry for a linear turbine cascade, 2016, V02BT38A011, https://doi.org/10.1115/GT2016-56268.
[28] J.C.R. Hunt, A.A. Wray, P. Moin, Eddies, Streams, and Convergence Zones in Turbulent Flows, Summer Program Center for Turbulence Research, 1998, pp. 193–207.
[29] C.B. Senel, H. Maral, L.A. Kavurmacioglu, C. Camci, An aerothermal study of the influence of squealer width and height near a hp turbine blade, Int. J. Heat Mass Transf. 120 (May 2018) 18–32, https://doi.org/10.1016/j.ijheatmasstransfer.2017.12.017.
[30] L.A. Kavurmacioglu, H. Maral, C.B. Senel, C. Camci, Performance of partial and cavity type squealer tip of a HP turbine blade in a linear cascade, Int. J. Aerosp. Eng. (ISSN 1687-5974) (2018), https://doi.org/10.1155/, Special Issue on “Advances in Aeroengines Technology (AAET)”, Hindawi Publ., in press.